

RESEARCH ARTICLE

Repository of MRI-derived models of the breast with single and multiple benign and malignant tumors for microwave imaging research

Ana C. Pelicano^{1,2}*, Maria C. T. Gonçalves^{1,2}, Tiago Castela³, M. Lurdes Orvalho³, Nuno A. M. Araújo^{2,4}, Emily Porter^{5,6}, Raquel C. Conceição^{1,2}, Daniela M. Godinho^{1,2}

1 Instituto de Biofísica e Engenharia Biomédica, Faculdade de Ciências, Universidade de Lisboa, Lisbon, Portugal, **2** Departamento de Física, Faculdade de Ciências, Universidade de Lisboa, Lisbon, Portugal, **3** Departamento de Radiologia, Hospital da Luz Lisboa, Luz Saúde, Lisboa, Portugal, **4** Centro de Física Teórica e Computacional, Faculdade de Ciências, Universidade de Lisboa, Lisbon, Portugal, **5** Chandra Family Department of Electrical and Computer Engineering, The University of Texas at Austin, Austin, TX, United States of America, **6** Department of Biomedical Engineering, McGill University, Montréal, Canada

* These authors contributed equally to this work.

* acpelicano@ciencias.ulisboa.pt



OPEN ACCESS

Citation: Pelicano AC, Gonçalves MCT, Castela T, Orvalho ML, Araújo NAM, Porter E, et al. (2024) Repository of MRI-derived models of the breast with single and multiple benign and malignant tumors for microwave imaging research. PLoS ONE 19(5): e0302974. <https://doi.org/10.1371/journal.pone.0302974>

Editor: Muhammad Zubair, Information Technology University, PAKISTAN

Received: October 30, 2023

Accepted: April 16, 2024

Published: May 17, 2024

Copyright: © 2024 Pelicano et al. This is an open access article distributed under the terms of the [Creative Commons Attribution License](https://creativecommons.org/licenses/by/4.0/), which permits unrestricted use, distribution, and reproduction in any medium, provided the original author and source are credited.

Data Availability Statement: The repository provides pre-processed T1-weighted MRI scans along with label maps containing segmented tissues. Furthermore, it includes an executable file that allows the integration of tissue dielectric properties within the models, spanning from 3 to 10 GHz. Access to the repository can be obtained via the following link: https://github.com/acpelicano/breast_models_repository.

Abstract

The diagnosis of breast cancer through MicroWave Imaging (MWI) technology has been extensively researched over the past few decades. However, continuous improvements to systems are needed to achieve clinical viability. To this end, the numerical models employed in simulation studies need to be diversified, anatomically accurate, and also representative of the cases in clinical settings. Hence, we have created the first open-access repository of 3D anatomically accurate numerical models of the breast, derived from 3.0T Magnetic Resonance Images (MRI) of benign breast disease and breast cancer patients. The models include normal breast tissues (fat, fibroglandular, skin, and muscle tissues), and benign and cancerous breast tumors. The repository contains easily reconfigurable models which can be tumor-free or contain single or multiple tumors, allowing complex and realistic test scenarios needed for feasibility and performance assessment of MWI devices prior to experimental and clinical testing. It also includes an executable file which enables researchers to generate models incorporating the dielectric properties of breast tissues at a chosen frequency ranging from 3 to 10 GHz, thereby ensuring compatibility with a wide spectrum of research requirements and stages of development for any breast MWI prototype system. Currently, our dataset comprises MRI scans of 55 patients, but new exams will be continuously added.

Introduction

MWI has been studied in the past decades for breast cancer screening and diagnosis [1–3]. Since then, new and improved systems continue to emerge with the purpose of bringing breast

Funding: This research was funded by Fundação para a Ciência e Tecnologia (FCT) (<https://www.fct.pt/en/>): - UI/BD/150762/2020 (<https://doi.org/10.54499/UI/BD/150762/2020>) awarded to ACP; - 2021.07228.BD (<https://doi.org/10.54499/2021.07228.BD>) awarded to MCTG; - UIDB/00645/2020 (<https://doi.org/10.54499/UIDB/00645/2020>) and UIDP/00645/2020 (<https://doi.org/10.54499/UIDP/00645/2020>) awarded to ACP, MCTG, DMG, and RCC; - UIDB/00618/2020 and UIDP/00618/2020 awarded to NAMA; - FCT/MET (PIDDAC) under the project 2022.08973.PTDC (<https://doi.org/10.54499/2022.08973.PTDC>) awarded to DMG and RCC. The funders had no role in study design, data collection and analysis, decision to publish, or preparation of the manuscript.

Competing interests: The authors have declared that no competing interests exist.

MWI technology closer to clinical settings [4–19]. Besides breast cancer detection, MWI has also shown potential in other areas such as breast cancer staging through axillary imaging [20], brain stroke detection [21], and bone health monitoring [22].

Anatomically accurate breast models are imperative for the development of breast MWI diagnostic systems, as well as microwave hyperthermia and ablation therapeutic devices [23, 24], as they allow systems to be designed, tested, and validated under conditions representative of patients and clinical examinations. Hence, numerical models of the breast must evolve and become increasingly more realistic, accurately portraying the complex structures of all normal, benign, and malignant tissues. MRI images have been largely used as the basis for the construction of anatomically realistic breast models [25–30]. Additionally, data extracted from these exams, such as voxel intensity, has been used to assign dielectric properties of biological tissues measured in large-scale patient studies [31, 32] to individual models through different strategies [26–28]. This results in the creation of dielectric property maps for breast tissues at microwave frequencies. The estimation of the dielectric properties of tissues using MRI images have also been studied before. To the best of the authors' knowledge, three different approaches that have been studied: one focusing on the acquisition of MRI sequences that can be used to determine the water content distribution of tissues, followed by the estimation of the dielectric properties of tissues based on this information [33, 34]; one concerning Electric Properties Tomography (EPT), which is based on B1 mapping and the estimation of tissues dielectric properties at the Larmor frequency [35–37], which can go up to 300 MHz; and finally, a recent strategy described in [38, 39] which combines the first two.

Most breast MWI research studies report highly accurate breast models concerning healthy breast tissues but oversimplified models of benign and malignant breast tumors [40–43]. These models are oftentimes unavailable to the scientific community, with only a few efforts made to build open-access repositories of breast models. Zastrow et al. [26] published a repository with nine anatomically realistic breast models derived from T1-weighted MRI images of healthy volunteers, containing seven tissue categories: glandular-high, glandular-median, glandular-low, fat-high, fat-median, fat-low, and transitional. Synthetic skin and muscle layers, with 1.5 mm and 0.5 cm thick respectively, were also added to the models. Later, Omer and Fear [44] made available a public repository of anthropomorphic breast models generated from 3.0T MRI images of healthy volunteers. The available five healthy breast models include realistic distributions of skin, fat, and fibroglandular tissue. Additionally, one diseased model containing a malignant tumor was derived from another 1.5T MRI scan and added to the repository. The tumor in this scan was segmented and made available as a separate model. Recently, a repository containing models of twenty-two breast cancer patients was made available for the development of breast cancer hyperthermia devices and treatment planning [45]. These models include anatomically accurate representations of skin, bone, fat, fibroglandular, and muscle tissues of both breasts, as well as malignant tumors.

In this paper, we introduce a new repository of anatomically realistic breast models for diagnostic and therapeutic microwave applications. Our models were derived from high-resolution T1-weighted MRI scans of patients with benign tumors and cancer patients, allowing modeling breast tumors with a high degree of realism regarding shape, dimension, location, and heterogeneity. Currently, models containing anatomical representations of skin, fat, fibroglandular, muscle, benign and malignant tumors from fifty-five patients have been made available; further efforts are being made to substantially increase the dataset. The repository offers a variety of breast models, which can be tumor-free or contain single or multiple tumors; combinations of multiple benign tumors, multiple malignant tumors, or combinations of both can be found in models with multiple tumors. It is worth noting that only six patient models include tumors in both breasts. We included breast tumors ranging in size from half

centimeter to eight centimeters, exhibiting diverse shapes (smoothness) and levels of heterogeneity. This repository includes the model files, allowing an easy reconfiguration of breast tissue models, if required; and an executable file enabling the generation of models that incorporate the dielectric properties of tissues for a chosen frequency value within the range of 3–10 GHz (with a step of 0.01 GHz), which fits investigators' needs and all developmental stages of any MWI prototype system. The developed repository can be accessed in [46].

Materials and methods

Dataset

The repository of anthropomorphic numerical models of the breast comprises MRI scans collected at Hospital da Luz-Lisboa between 09/25/2019 and 06/29/2022—clinical studies under references CES/44/2019/ME and CES/34/2020/ME. A written informed consent was obtained from all participants and exams were anonymized before processing. Patients were scanned in a prone position using a 3.0T MAGNETON Vida clinical magnetic resonance scanner (Siemens Healthineers, Erlangen, Germany) with a dedicated breast coil (Siemens Breast 18 coil, Siemens Healthineers, Erlangen, Germany). Two MRI sequences were used: the direct coronal isotropic three-dimensional (3D) T1-weighted (T1-w) Fast Low Angle Shot 3D (f3D) Volumetric Interpolated Breath-hold Examination (VIBE) Dixon image sequence (T1-w Dixon), which allows obtaining four sets of images: in-phase (I), out-of-phase (O), fat-only (F), and water-only images (W); and the Dynamic Contrast Enhanced (DCE) transversal 3D T1-w Fast f3D Spectral Attenuated Inversion Recovery (SPAIR) sequence, which consists of six sets of images—a pre-contrast image acquired before the injection of intravenous gadolinium, and five post-contrast images. Moreover, digital subtractions of each post-contrast image from the pre-contrast image were also obtained to enhance tumors and annul hypersignal regions previously present in pre-contrast images.

This repository includes scans from patients with breast tumors scored by a radiologist with BI-RADS 2 and 3, and with BI-RADS 5 and 6 [47], which were classified as benign tumors and malignant tumors, respectively. Currently, the repository includes exams of 55 patients with a total of 84 breast tumors: 46 benign and 38 malignant; new exams will be added as the processing of each exam is completed.

Model processing

To create 3D anatomically realistic models of the breast, two MRI sequences were used for tissue segmentation. T1-w Dixon-I and T1-w Dixon-F images were used for fat, fibroglandular, skin and muscle segmentation, and a subtraction image obtained from the T1-w DCE-f3D sequence was used to segment the breast tumors. Image registration using the Insight Toolkit (ITK) implementation (SimpleITK) [48] was performed to align and correctly superimpose the two sequences. For all images, the pre-processing pipeline included the correction of the bias field via SimpleITK N4BiasFieldCorrectionImageFilter implementation [49], followed by Minimum-Maximum data normalization [50] and a median filtering step for noise removal and edge smoothing [51, 52]. For scans with infra-centimetric tumors, the median filtering step was removed from the pre-processing pipeline, otherwise the original size and shape of the tumors would be compromised.

Data processing includes: (1) the estimation of the sternum position using the T1-w Dixon-W images; (2) the use of the sternum position as the seed for the region growing algorithm which is applied to the T1-w Dixon-F images in order to separate fat tissue of the breast region from fat tissue from the thoracic cavity; (3) the dilation of the resulting fat mask using a structuring element of radius 3 and whitening out of the anterior part of the body to include fat,

skin and fibroglandular tissue, resulting in a mask of the entire breast region; (4) the dilation of the anterior and posterior part of the breast contour to obtain the final skin and muscle masks, respectively; (5) the use of a Gaussian Mixture Model to separate the fat tissue from the fibroglandular tissue using the T1-w Dixon-I images [26]. Additionally, these two categories (fat and fibroglandular) were each further subdivided into: low, medium, and high according to voxel intensity, allowing to incorporate further tissue heterogeneity. Region growing [53] and Hoshen-Kopelman [54] algorithms were applied to pre-processed subtraction images from the DCE-fl3D sequence for tumor segmentation. Details regarding breast model processing are described in [55].

Dielectric properties assignment

The dielectric properties of segmented tissues were determined using a piecewise linear interpolation method, inspired by [26]. This approach facilitated the mapping of the T1-w Dixon-W voxel intensities to the tissue's dielectric property curves. It is important to note that T1-w Dixon-W signal intensities are directly proportional to the amount of hydrogen nuclei in the tissues, implying that higher voxel intensities correspond to greater water content in the tissues [56].

For fat, fibroglandular, skin, and muscle tissues, the Debye parameters used for the relative permittivity and conductivity curves are well-documented in the literature [57]. To account for tissue heterogeneity in our models, a 5% dielectric variation was introduced with respect to the nominal properties for skin and muscular tissue. The generated upper and lower bound curves for muscle and skin were subsequently assigned to the highest and lowest intensity voxels present in the segmented tissues, respectively. The remaining voxels within the segmented tissues were linearly mapped to a value between the curves, via a piece-wise linear strategy previously described in [26].

The 1-pole Cole-Cole parameters of the malignant tumors dielectric property curves are available in [32]. These parameters were subsequently converted into Debye parameters, as detailed in [55]. Benign breast tumors and breast tissues with low adipose content exhibit similar dielectric properties [32]. Consequently, we assumed that the dielectric properties of benign tumors fall within the range defined by the fibroglandular curves. Fig 1 illustrates the dielectric property curves for all breast tissues within the 3-10 GHz range.

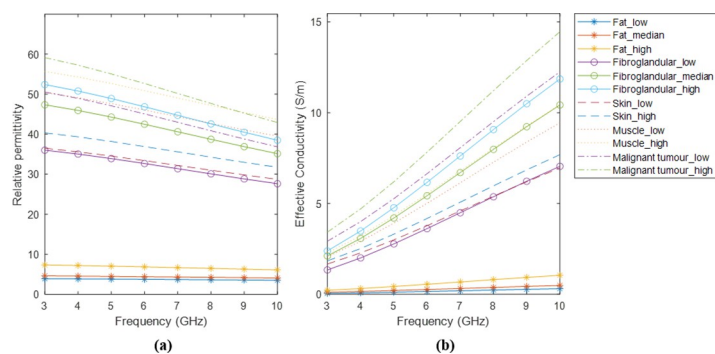


Fig 1. Dielectric property curves of normal breast tissues and tumors for frequencies between 3-10 GHz. (a) Relative permittivity curves. (b) Effective conductivity curves.

<https://doi.org/10.1371/journal.pone.0302974.g001>

Repository

Our repository is divided into folders, one per patient. So far, we were able to populate the database with exams from 55 patients. Each folder is identified with patient ID and contains the pre-processed T1-w Dixon-W image (with $0.9965 \times 0.9965 \times 1 \text{ mm}^3$ spatial resolution) of the patient, and two maps with labelled tissue types, identified as 'Label_map_simple' and 'Label_map_detailed'. In 'Label_map_simple', we present a simplification of the breast, considering only benign breast tumors (label -4), malignant tumors (label -3), skin (label -2), muscle (label -1), background (label 0), and a combination of fat+fibroglandular tissue (label 1), i.e., the breast is assumed to be composed of fat, and fibroglandular tissue is disregarded. In 'Label_map_detailed', in addition to benign and malignant breast tumors, skin, muscle and background, we also include three sub-categories of fat and fibroglandular tissues according to voxel intensity, as well as a transitional tissue between these two tissue types in the label map, following the rationale in Zastrow et al. [26]. The new labels of the segmented tissues are the following: benign breast tumors (label -4), malignant tumors (label -3), skin (label -2), muscle (label -1), background (label 0), fibroglandular_low (label 1), fibroglandular_median (label 2), fibroglandular_high (label 3), transition (label 4), fat_low (label 5), fat_median (label 6), and fat_high (label 7). All images are available in MetaImage Medical Format MHA file format. Furthermore, information such as the Body Mass Index (BMI), and breast tumor location, number, type, and dimension per patient is given. In exams with more than one breast tumor with the same classification, tumors are referred to as 'XS—extra small size', 'S—small size', 'M—medium size', 'L—large size', and 'XL—extra large size' according to their relative dimensions. The tumors vary in size between approximately 0.5 cm and 8 cm.

Additionally, the repository also provides an executable file—the 'dielectric_properties_assignment.exe'—which allows researchers to obtain the relative permittivity and effective conductivity maps of all exams for a specific frequency in the range of 3 to 10 GHz, with a step of 0.01 GHz. These dielectric property maps are available both in MHA and MATLAB file formats.

Results and discussion

The developed repository provides bilateral models of the breast region, including benign and malignant breast tumors. Cases with multiple tumors are also available to increase the set of scenarios provided to microwave imaging studies. Fig 2 shows some examples of breast models with multiples tumors that are available in the repository [46].

Good practices for the use of our repository include the download of the images and the executable file in the same directory. When opening the 'dielectric_properties_assignment.exe' file, the exam selection window will pop up as shown in Fig 3. Fig 4 is an example of a T1-w Dixon-W image and the corresponding simple label map.

After selecting the exam, researchers should choose the desired label map as soon as the second window pops up, as depicted in Fig 5. Please be aware that customized label maps, tailored to meet the specific requirements of researchers, can be created by modifying the labels associated with segmented tissues from the provided label maps.

A frequency value between 3 and 10 GHz, with a step of 0.01 GHz can be chosen in the third pop-up window, as shown in Fig 6. This feature allows the generation of multiple numerical models containing tissue dielectric properties that match the interests of researchers in the medical MWI field.

Researchers can save the relative permittivity and effective conductivity maps by selecting "Yes" in the fourth pop-up window. An illustration is shown in Fig 7.

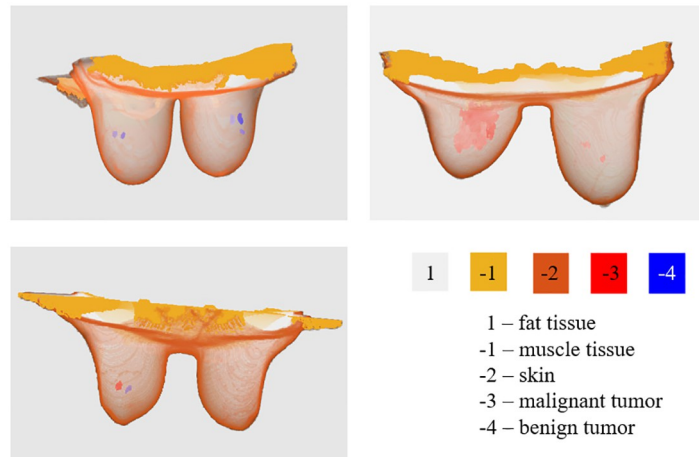


Fig 2. Examples of breast models with multiple tumors available in the repository. Exams 31 (top left) and 2 (top right) include only benign and malignant tumors in both breasts, respectively. Exam 4 (bottom left) exhibits a malignant and a benign tumor in one breast, and a healthy breast.

<https://doi.org/10.1371/journal.pone.0302974.g002>

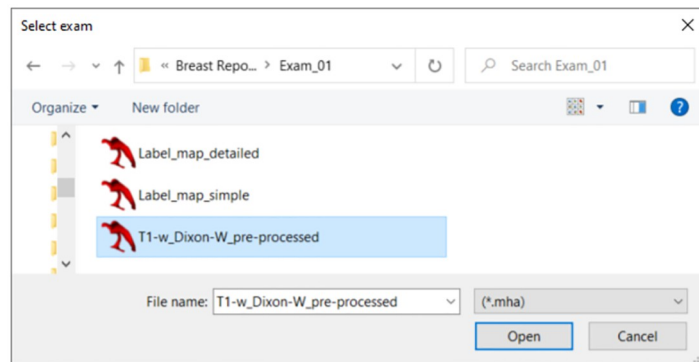


Fig 3. Exam selection window of the executable file.

<https://doi.org/10.1371/journal.pone.0302974.g003>

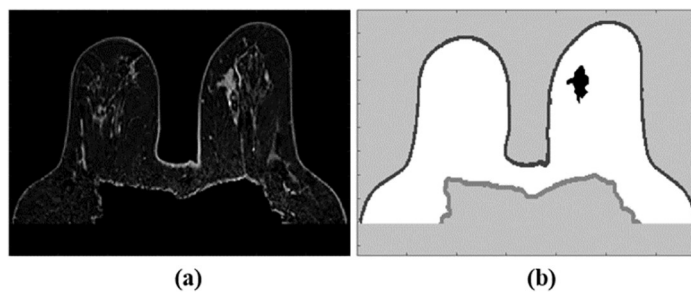


Fig 4. Example of a MRI exam and corresponding label map (Exam 11 of the repository). (a) Axial view of a T1-w_Dixon-W_pre-processed image. (b) Axial view of the corresponding Label_map_simple.

<https://doi.org/10.1371/journal.pone.0302974.g004>

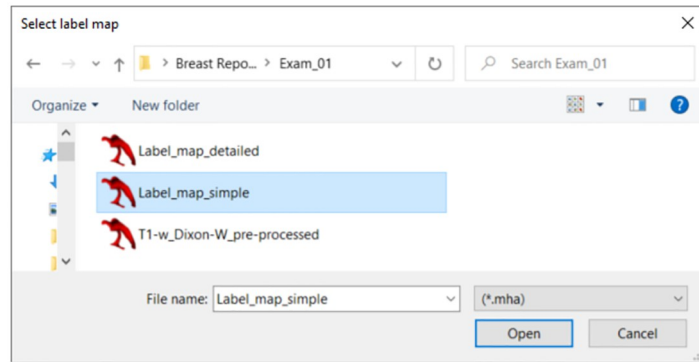


Fig 5. Label map selection window of the executable file.

<https://doi.org/10.1371/journal.pone.0302974.g005>

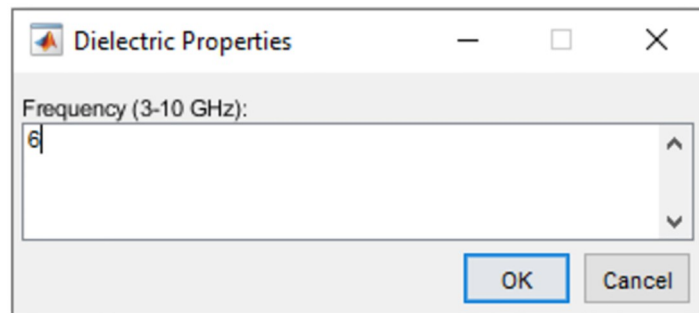


Fig 6. Frequency selection window of the executable file.

<https://doi.org/10.1371/journal.pone.0302974.g006>

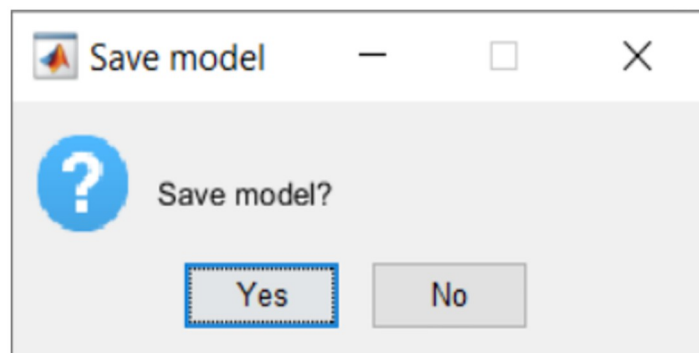


Fig 7. Save model window of the executable file.

<https://doi.org/10.1371/journal.pone.0302974.g007>

If the “Yes” button is selected in Fig 7, the maps of relative permittivity and effective conductivity will be saved in the ‘SavedFiles’ folder of that same directory and under the name Permittivity_Matrix_’freq’_’date’_’time’ and Conductivity_Matrix_’freq’_’date’_’time’, respectively. ‘freq’ stands for the chosen frequency and ‘date’ and ‘time’ are set automatically at the moment of saving. Fig 8 shows the dielectric properties maps for a frequency of 6 GHz.

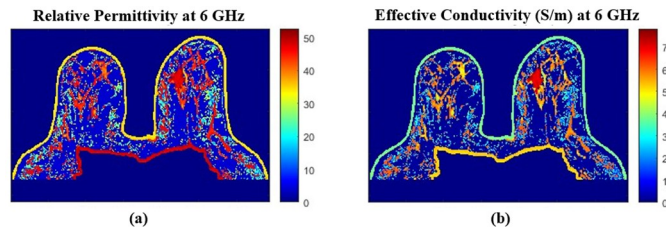


Fig 8. Dielectric property maps for a frequency of 6 GHz. (a) Axial view of the relative permittivity map for a frequency of 6 GHz. (b) Axial view of the effective conductivity map for a frequency of 6 GHz.

<https://doi.org/10.1371/journal.pone.0302974.g008>

Conclusions

In this paper, we present a new open-access repository of MRI-derived numerical breast models containing normal breast tissues, as well as benign and malignant tumors, suitable for MWI purposes. Note that the available models can be utilized for alternative applications, for example MW hyperthermia, provided that the appropriate properties are attributed to the tissue maps. The patient models encompass both breasts, wherein a minimum of one breast contains at least one tumor. Dielectric property maps for frequencies between 3 and 10 GHz can be generated through an executable file available in the repository. This is also the first repository reporting benign tumors, and providing models with multiple tumors, allowing for complex and realistic test scenarios needed for feasibility and performance assessment of MWI devices. Currently, fifty-five patient models are available; further efforts are being made to substantially increase the dataset.

Acknowledgments

The authors acknowledge the study with references CES/44/2019/ME and CES/34/2020/ME in Hospital da Luz Lisboa and the technicians for the MRI acquisitions.

Author Contributions

Conceptualization: Ana C. Pelicano, Maria C. T. Gonçalves, Raquel C. Conceição, Daniela M. Godinho.

Data curation: Ana C. Pelicano, Maria C. T. Gonçalves, Daniela M. Godinho.

Formal analysis: Ana C. Pelicano, Maria C. T. Gonçalves.

Funding acquisition: Ana C. Pelicano, Maria C. T. Gonçalves, Nuno A. M. Araújo, Raquel C. Conceição, Daniela M. Godinho.

Investigation: Ana C. Pelicano, Maria C. T. Gonçalves.

Methodology: Ana C. Pelicano, Maria C. T. Gonçalves, Daniela M. Godinho.

Project administration: Raquel C. Conceição.

Resources: Tiago Castela, M. Lurdes Orvalho.

Software: Ana C. Pelicano, Maria C. T. Gonçalves, Daniela M. Godinho.

Supervision: Nuno A. M. Araújo, Emily Porter, Raquel C. Conceição, Daniela M. Godinho.

Validation: Ana C. Pelicano, Maria C. T. Gonçalves.

Visualization: Ana C. Pelicano, Maria C. T. Gonçalves.

Writing – original draft: Ana C. Pelicano.

Writing – review & editing: Maria C. T. Gonçalves, Tiago Castela, M. Lurdes Orvalho, Nuno A. M. Araújo, Emily Porter, Raquel C. Conceição, Daniela M. Godinho.

References

1. Hagness SC, Taflove A, Bridges JE. Two-dimensional FDTD analysis of a pulsed microwave confocal system for breast cancer detection: fixed-focus and antenna-array sensors. *IEEE Trans Biomed Eng.* 1999; 45(12):1470–1479. <https://doi.org/10.1109/10.730440>
2. Fasoula A, Duchesne L, Cano JDG, Lawrence P, Robin G, Bernard J-G. On-site validation of a microwave breast imaging system, before first patient study. *Diagnostics.* 2018; 8(53):1–38. <https://doi.org/10.3390/diagnostics8030053> PMID: 30126213
3. Solis-Nepote M, Reimer T, Pistorius S. An air-operated bistatic system for breast microwave radar imaging: pre-clinical validation. *Annu Int Conf IEEE Eng Med Biol Soc. Berlin, Germany.* 2019:1859–1862.
4. Bourqui J, Sill JM, Fear EC. A prototype system for measuring microwave frequency reflections from the breast. *Int J Biomed Imag.* 2012; 2012:1–12. <https://doi.org/10.1155/2012/562563>
5. Meaney PM, Fanning MW, Li D, Poplack SP, Paulsen KD. A clinical prototype for active microwave imaging of the breast. *IEEE Trans Microw Theory Tech.* 2000; 48(11):1841–1853. <https://doi.org/10.1109/22.883861>
6. Meaney PM, Fanning MW, Reynolds T, Fox CJ, Fang Q, Kogel CA, et al. Initial clinical experience with microwave breast imaging in women with normal mammography. *Acad Radiol.* 2007; 14(2):207–218. <https://doi.org/10.1016/j.acra.2006.10.016> PMID: 17236994
7. Henriksson T, Klemm M, Gibbins D, Leendertz J, Horseman T, Preece AW, et al. Clinical trials of a multistatic UWB radar for breast imaging. in *Proc Loughborough Antennas Propag Conf (LAPC)*. Loughborough, UK. 2011 Nov:1–4.
8. Lavoie BR, Bourqui J, Fear EC, Okoniewski M. Metrics for assessing the similarity of microwave breast imaging scans of healthy volunteers. *IEEE Trans Med Imag.* 2018; 37(8):1788–1798. <https://doi.org/10.1109/TMI.2018.2806878> PMID: 29994630
9. Porter E, Coates M, Popović M. An early clinical study of time-domain microwave radar for breast health monitoring. *IEEE Trans Biomed Eng.* 2016; 63(3):530–539. <https://doi.org/10.1109/TBME.2015.2465867> PMID: 26259214
10. Yang F, Sun L, Hu Z, Wang H, Pan D, Wu R, et al. A large-scale clinical trial of radar-based microwave breast imaging for Asian women: phase I. *IEEE AP.S/URSI.* San Diego, CA, USA. 2017 July:781–783.
11. Shere M, Lyburn I, Sidebottom R, Massey H, Gillett C, Jones L. MARIA[®] M5: A multicentre clinical study to evaluate the ability of the Micrima radio-wave radar breast imaging system (MARIA[®]) to detect lesions in the symptomatic breast. *Eur J Rad.* 2019; 116:61–67. <https://doi.org/10.1016/j.ejrad.2019.04.017> PMID: 31153575
12. Fasoula A, Duchesne L, Moloney BM, Cano JDG, Chenot C, Oliveira BL, et al. Pilot patient study with the Wavelia Microwave Breast Imaging system for breast cancer detection: Clinical feasibility and identified technical challenges. *14th Eur Conf Antennas Propag (EuCAP)*. Copenhagen, Denmark. 2020 Mar:1–5.
13. Moloney BM, MCanena PF, Elwahas SMW, Fasoula A, Duchesne L, Cano JDG, et al. The Wavelia Microwave Breast Imaging system—tumour discriminating features and their clinical usefulness. *Br J Radiol.* 2021; 94(1128):1–12. <https://doi.org/10.1259/bjr.20210907> PMID: 34581186
14. Sani L, Vispa A, Loretoni R, Duranti M, Ghavami N, Sánchez-Bayueta DA, et al. Breast lesion detection through MammoWave device: Empirical detection capability assessment of microwave images' parameters. *PLoS ONE.* 2021; 16(4):e0250005. <https://doi.org/10.1371/journal.pone.0250005>
15. Sani L, Vispa A, Ghavami N, Sánchez-Bayueta DA, Badia M, Bigotti A, et al. MammoWave breast imaging device: a procedure for device's characterization via phantom measurements and subsequent clinical trials' preliminary results. *IEEE CAMA. Antibes Juan-les-Pins, France.* 2021 Nov:483–486.
16. Sánchez-Bayueta DA, Ghavami N, Castellano CR, Bigotti A, Badia M, Papini L, et al. A multicentric, single arm, prospective, stratified clinical investigation to confirm mammoWave's ability in breast lesions detection. *Diagnostics.* 2023; 13(12):2100. <https://doi.org/10.3390/diagnostics13122100>
17. Janjic A, Cayoren M, Akduman I, Yilmaz T, Onemli E, Bugdayci O, et al. SAFE: A novel microwave imaging system design for breast cancer screening and early detection—clinical evaluation. *Diagnostics.* 2021; 11(3):533. <https://doi.org/10.3390/diagnostics11030533> PMID: 33809770

18. Janjic A, Akduman I, Cayoren M, Bugdayci O, Aribal ME. Gradient-boosting algorithm for microwave breast lesion classification—SAFE clinical investigation. *Diagnostics*. 2022; 12(12):3151. <https://doi.org/10.3390/diagnostics12123151> PMID: 36553158
19. Janjic A, Akduman I, Cayoren M, Bugdayci O, Aribal ME. Microwave breast lesion classification—results from clinical investigation of the SAFE microwave breast cancer system. *Acad Radiol*. 2023; 30(S2):S1–S8. <https://doi.org/10.1016/j.acra.2022.12.001> PMID: 36549991
20. Godinho DM, Felício JM, Fernandes CA, Conceição RC. Experimental evaluation of an axillary microwave imaging system to aid breast cancer staging. *IEEE J Electromagn RF Microw Med Biol*. 2022; 6(1):68–76. <https://doi.org/10.1109/JERM.2021.3097877>
21. Vasquez JA, Scapatucci R, Turvani G, Bellizzi G, Rodriguez-Duarte DO, Joachimowicz N, et al. A prototype microwave system for 3D brain stroke imaging. *Sensors*. 2020; 20(9):2607. <https://doi.org/10.3390/s20092607>
22. Amin B, Shahzad A, O'Halloran M, Elahi MA. Microwave bone imaging: A preliminary investigation on numerical bone phantoms for bone health monitoring. *Sensors*. 2020; 20(21):6320. <https://doi.org/10.3390/s20216320> PMID: 33167562
23. Datta NR, Ordóñez SG, Gaipi US, Paulides MM, Crezee H, Gellermann J, et al. Local hyperthermia combined with radiotherapy and/or chemotherapy: Recent advances and promises for the future. *Cancer Treat Rev*. 2015; 41:742–753. <https://doi.org/10.1016/j.ctrv.2015.05.009> PMID: 26051911
24. Brace CL. Microwave tissue ablation: Biophysics, technology, and applications. *Crit Rev Biomed Eng*. 2010; 38:65–78. <https://doi.org/10.1615/critrevbiomedeng.v38.i1.60> PMID: 21175404
25. Li X, Hagness SC. A confocal microwave imaging algorithm for breast cancer detection. *IEEE MWCL*. 2001; 11(3):130–132.
26. Zastrow E, Davis SK, Lazebnik M, Kelcz F, Van Veen BD, Hagness SC. Development of anatomically realistic numerical breast phantoms with accurate dielectric properties for modeling microwave interactions with the human breast. *IEEE Trans Biomed Eng*. 2008; 55:2792–2800.
27. Zhu G, Oreshkin B, Porter E, Coates M, Popović M. Numerical breast models for commercial FDTD simulators. 3rd Eur Conf Antennas Propag (EuCAP). Berlin, Germany. 2009 Mar:263–267.
28. Tunçay AH, Akduman I. Realistic microwave breast models through T1-weighted 3-D MRI data. *IEEE Trans Biomed Eng*. 2015; 62(2):688–698. <https://doi.org/10.1109/TBME.2014.2364015> PMID: 25347868
29. Omer M, Fear EC. Automated 3D method for the construction of flexible and reconfigurable numerical breast models from MRI scans. *Med Biol Eng Comput*. 2018; 56(6):1027–1040. <https://doi.org/10.1007/s11517-017-1740-9> PMID: 29130138
30. Lu M, Xiao X, Song H, Liu G, Lu H, Kikkawa T. Accurate construction of 3-D numerical breast models with anatomical information through MRI scans. *Comput Biol Med*. 2021; 130(104):104205. <https://doi.org/10.1016/j.combiomed.2020.104205> PMID: 33421826
31. Lazebnik M, McCartney L, Popovic D, Watkins CB, Lindstrom MJ, Harter J, et al. A large-scale study of the ultrawideband microwave dielectric properties of normal breast tissues obtained from reduction surgeries. *Phys Med Biol*. 2007; 52(10):2637–2656. <https://doi.org/10.1088/0031-9155/52/10/001> PMID: 17473342
32. Lazebnik M, Popovic D, McCartney L, Watkins CB, Lindstrom MJ, Harter J, et al. A large-scale study of the ultrawideband microwave dielectric properties of normal, benign and malignant breast tissues obtained from cancer surgeries. *Phys Med Biol*. 2007; 52(20):6093–6115. <https://doi.org/10.1088/0031-9155/52/20/002> PMID: 17921574
33. Neeb H, Dierkes T, Shah NJ. Quantitative T1 mapping and absolute water content measurement using MRI. *International Congress Series*. 2004; 1265:113–123. <https://doi.org/10.1016/j.ics.2004.02.168>
34. Laurita R, Cavagnaro M, Frezza F, Tannino M. Evaluation of tissue dielectric properties from MR images. 6th UK, Europe, China Millimeter Waves and THz Technology Workshop (UCMMT). Rome, Italy. 2013 Sept:1–2.
35. Katscher U, Hanft M, Vernickel P, Findekle C. Experimental verification of Electric Properties Tomography (EPT). 14th Annual Meeting ISMRM. Seattle, WA, USA. 2006 May:3035.
36. Katscher U, Dornik T, Findekle C, Vernickel P, Nehrke K. In vivo determination of electric conductivity and permittivity using a standard MR system. In: Scharfetter H, Merwa R, editors. 13th IFMBE Proceedings. Springer, Berlin, Heidelberg; 2007. pp. 508–511.
37. Katscher U, Voigt T, Findekle C, Vernickel P, Nehrke K, Dössel O. Determination of electric conductivity and local SAR via B1 mapping. *IEEE Trans Med Imaging*. 2009; 28(9):1365–1374. <https://doi.org/10.1109/TMI.2009.2015757> PMID: 19369153
38. Liporace F, Cavagnaro M. Wideband dielectric properties reconstruction from MR acquisition. 17th EuCAP. Florence, Italy. 2023 March:1–4.

39. Liporace F, Cavagnaro M. Development of MR-based procedures for the implementation of patient-specific dielectric models for clinical use. *J. Mech. Med. Biol.* 2023; 23(6):2340031. <https://doi.org/10.1142/S0219519423400316>
40. Shea JD, Kosmas P, Van Veen BD, Hagness SC. Contrast-enhanced microwave imaging of breast tumours: a computational study using 3D realistic numerical phantoms. *Inverse Probl.* 2010; 26. <https://doi.org/10.1088/0266-5611/26/7/074009> PMID: 20936053
41. Zhu X, Zhao Z, Wang J, Chen G, Liu QH. Active adjoint modeling method in microwave induced thermoacoustic tomography for breast tumor. *IEEE Trans Biomed Eng.* 2014; 61:1957–1966. <https://doi.org/10.1109/TBME.2014.2309912> PMID: 24956614
42. Amdaouch I, Aghzout O, Naghar A, Alejos AV, Falcone FJ. Breast tumor detection system based on a compact UWB antenna design. *PIER M.* 2018; 64:123–133. <https://doi.org/10.2528/PIERM17102404>
43. Chen B, Shorey J, Saunders RS Jr, Richard S, Thompson J, Nolte LW, et al. An anthropomorphic breast model for breast imaging simulation and optimization. *Acad Radiol.* 2011; 18:536–546. <https://doi.org/10.1016/j.acra.2010.11.009> PMID: 21397528
44. Omer M, Fear EC. Anthropomorphic breast model repository for research and development of microwave breast imaging technologies. *Sci Data.* 2018; 5:1–10. <https://doi.org/10.1038/sdata.2018.257> PMID: 30457568
45. Androulakis I, Sumser K, Machielse MND, Koppert L, Jager A, Nout R, et al. Patient-derived breast model repository, a tool for hyperthermia treatment planning and applicator design. *Int J Hyperth.* 2022; 39:1213–1221. <https://doi.org/10.1080/02656736.2022.2121862> PMID: 36104074
46. Pelicano AC, Gonçalves MCT, Godinho DM, Castela T, Orvalho ML, Araújo NAM, et al. Breast Models Repository for Electromagnetic Applications. 2023. Available from: https://github.com/acpelicano/breast_models_repository.
47. D’Orsi C, Sickles E, Mendelson E, Morris E. ACR BI-RADS® Atlas, Breast Imaging Reporting and Data System. 5th ed. Reston, VA, USA: American College of Radiology; 2013.
48. Yaniv Z, Lowekamp BC, Johnson HJ, Beare R. SimpleITK Image-Analysis Notebooks: A Collaborative Environment for Education and Reproducible Research. *J Digit Imaging.* 2018; 31:290–303. <https://doi.org/10.1007/s10278-017-0037-8>
49. Tustison NJ, Avants BB, Cook PA, Zheng Y, Egan A, Yushkevich PA, et al. N4ITK: Improved N3 bias correction. *IEEE Trans Med Imaging.* 2010; 29:1310–1320. <https://doi.org/10.1109/TMI.2010.2046908> PMID: 20378467
50. Patro S, Sahu K. Normalization: A preprocessing stage. arXiv:1503.06462v1. 2015. Available from: <https://arxiv.org/abs/1503.06462>.
51. Ali H. MRI medical image denoising by fundamental filters. *SCIREA J Comput.* 2017; 2:12–26.
52. Gonzalez RC, Woods RE. *Digital Image Processing.* Hoboken, NJ, USA: Prentice Hall; 2002.
53. Kroon D. Region Growing (version 1.0.0.0), MATLAB Central File Exchange. 2023. Available from: <https://www.mathworks.com/matlabcentral/fileexchange/19084-region-growing>.
54. Hoshen J, Kopelman R. Percolation and cluster distribution. I. Cluster multiple labeling technique and critical concentration algorithm. *Phys Rev B.* 1976; 14:3438–3445. <https://doi.org/10.1103/PhysRevB.14.3438>
55. Pelicano AC, Gonçalves MCT, Godinho DM, Castela T, Orvalho ML, Araújo NAM, et al. Development of 3D MRI-based anatomically realistic models of breast tissues and tumours for microwave imaging diagnosis. *Sensors.* 2021; 21(24):8265. <https://doi.org/10.3390/s21248265> PMID: 34960354
56. Godinho DM, Felício JM, Castela T, Silva NA, Orvalho ML, Fernandes CA, et al. Development of MRI-based axillary numerical models and estimation of axillary lymph node dielectric properties for microwave imaging. *Med Phys.* 2021; 48(10):5974–5990. <https://doi.org/10.1002/mp.15143> PMID: 34338335
57. Zastrow E, Davis SK, Lazebnik M, Kelcz F, Van Veen BD, Hagness SC. Database of 3D Grid-Based Numerical Breast Phantoms for Use in Computational Electromagnetics Simulations. Available from: <https://uwcem.ece.wisc.edu/MRI/database/InstructionManual.pdf>.